Nanofabricated upconversion nanoparticles for photodynamic therapy

Baris Ungun,[1] Robert K. Prud'homme,[2] Stephanie J. Budijono[1], Jingning Shan[2], Shuang Fang Lim[2,3], Yiguang Ju[2], and Robert Austin[3]
[1]Department of Chemical Engineering, Princeton University, Princeton, NJ, USA
[2]Department of Mechanical and Aerospace Engineering, Princeton University, Princeton, NJ, USA

[3]Department of Physics, Princeton University, Princeton, NJ, USA
[*]Corresponding author: rha@princeton.edu

Abstract: We present a novel process for the production of three-layer Composite Nanoparticles (CNPs) in the size range 100-300 nm with an up-converting phosphor interior, a coating of porphyrin photosensitizer, and a biocompatible PEG outer layer to prevent clearance by the reticuloendothelial system. We show that these CNPs produce millimolar amounts of singlet oxygen at NIR intensities far less than other two-photon techniques.

OCIS codes: (170.0170) Medical Optics and Biotechnology

References and links

1. S. Heer, K. Kompe, H. U. Gudel, and M. Haase, "Highly efficient multicolour upconversion emission in transparent colloids of lanthanide-doped NaYF4 nanocrystals," Adv. Mat. **16**, 2102-+ (2004).
2. K. Kuningas, T. Rantanen, U. Karhunen, T. Lovgren, and T. Soukka, "Simultaneous use of time-resolved fluorescence and anti-stokes photoluminescence in a bioaffinity assay," Anal. Chem. **77**, 2826-2834 (2005).
3. K. van de Rijke, H. Zijlmans, S. V. Li, T. A. K. Raap, R. S. Niedbala, and H. J. Tanke, "Up-converting phosphor reporters for nucleic acid microarrays," Nature Biotech. **19**, 273-276 (2001).
4. M. Zuiderwijk, H. J. Tanke, R. S. Niedbala, and P. Corstjens, "An amplification-free hybridization-based DNA assay to detect Streptococcus pneumoniae utilizing the up-conversion phosphor technology," Clin. Biochem. **36**, 401-403 (2003).
5. S. F. Lim, R. Riehn, W. S. Ryu, N. Khanarian, C. K. Tung, D. Tank, and R. H. Austin, "In vivo and scanning electron microscopy imaging of upconverting nanophosphors in Caenorhabditis elegans," Nano Lett. **6-2** (2006).
6. V. P. Torchilin, and V. S. Trubetskoy, "Which Polymers Can Make Nanoparticulate Drug Carriers Long-Circulating," Adv. Drug Del. Rev. **16**, 141-155 (1995).
7. J. Shan and Y. G. Ju, "Synthesis, characterization and SiO_2 coating of NaF_4Y:Er3+ upconversion nanophosphors using high temperature ligands," Adv. Mat. Submitted (2007).
8. B. K. Johnson and R. K. Prud'homme, "Flash NanoPrecipitation of organic actives and block copolymers using a confined impinging jets mixer," Australian J. Chem. **56**, 1021-1024 (2003).
9. F. Auzel, "Upconversion and anti-stokes processes with f and d ions in solids," Chem. Rev. **104**, 139-173 (2004).
10. M. J. Moreno, E. Monson, R. G. Reddy, A. Rehemtulla, B. D. Ross, M. Philbert, R. J. Schneider, and R. Kopelman, "Production of singlet oxygen by Ru(dpp(SO3)(2))(3) incorporated in polyacrylamide PEBBLES," Sens. Actuat. B-Chem. **90**, 82-89 (2003).
11. B. A. Lindig, M. A. J. Rodgers, and A. P. Schaap, "Determination of the Lifetime of Singlet Oxygen in D2o Using 9,10-Anthracenedipropionic Acid, a Water-Soluble Probe," J. Am. Chem. Soc. **102**, 5590-5593 (1980).
12. D. K. Chatterjee and Z. Yong, "Upconverting nanoparticles as nanotransducers for photodynamic therapy in cancer cells," Nanomed. **3**, 73-82 (2008).
13. S. M. Ansell, S. A. Johnstone, P. G. Tardi, L. Lo, S. W. Xie, Y. Shu, T. O. Harasym, N. L. Harasym, L. Williams, D. Bermudes, B. D. Liboiron, W. Saad, R. K. Prud'homme, and L. D. Mayer, "Modulating the therapeutic activity of nanoparticle delivered paclitaxel by manipulating the hydrophobicity of prodrug conjugates," J. Med. Chem. **51**, 3288-3296 (2008).
14. P. Zhang, W. Steelant, M. Kumar, and M. Scholfield, "Versatile photosensitizers for photodynamic therapy at infrared excitation," J. Am. Chem. Soc. **129**, 4526 (2007).
15. H. Maeda, J. Fang, T. Inutsuka, and Y. Kitamoto, "Vascular permeability enhancement in solid tumor: various factors, mechanisms involved and its implications," Int. Immunopharm. **3**, 319-328 (2003).

#103213 - $15.00 USD Received 27 Oct 2008; revised 8 Dec 2008; accepted 10 Dec 2008; published 22 Dec 2008

16. M. E. Gindy, S. Ji, T. R. Hoye, A. Z. Panagiotopoulos, and R. K. Prud'homme, "Preparation of Poly(ethylene glycol) Protected Nanoparticles with Variable Bioconjugate Ligand Density," Biomacromol. **9**, 2705-2711 (2008).
17. M. E. Gindy, A. Z. Panagiotopoulos, and R. K. Prud'homme, "Composite block copolymer stabilized nanoparticles: Simultaneous encapsulation of organic actives and inorganic nanostructures," Langmuir **24**, 83-90 (2008).
18. Y. Liu, K. Kathan, W. Saad, and R. K. Prud'homme, "Ostwald ripening of beta-carotene nanoparticles," Phys. Rev. Lett. **98** (2007).

1. Introduction

Up-conversion phosphors (UCPs) are ceramic materials in which rare earth atoms are embedded in a crystalline matrix. The materials absorb infrared radiation and up-convert to emit in the visible spectrum through a series of real as opposed to virtual levels as in conventional two-photon dyes. The upconversion mechanism can be described as either sequential excitation of the same atom or excitation of two centers and subsequent energy transfer [1-4]. The emission of UCPs consists of sharp lines characteristic of atomic transitions in a well-ordered matrix. By use of different rare earth dopants, including Er^{3+}, a large number of distinctive emission spectra can be obtained that can be tailored to the photosensitizer excitation spectra. Their main advantage is the sequential 2 (or higher) photon nature of the excitation process, which gives rise to the very low power levels associated with upconversion. The excitation intensities we use here of Watts/mm^2 are 10^7 times less than the intensities needed for 2-photon excitation of typical organic dyes[5]. The adsorption maximum of the Er^{3+} ion is centered at 975 nm and is ideally suited for photodynamic therapy (PDT) since it can be easily excited using very low cost IR CW diode lasers, and it falls in a region of relative transparency for penetration in tissue. Another advantage of UCPs is their resistance to photobleaching. Since these transitions come from rare earth atomic orbitals and not molecular orbitals UCPs do not photobleach as do organic dyes, we have illuminated these materials for days at high levels of emission output and not observed any decrease in the effective quantum yield. Since they emit from the inner I-shell levels of the rare earths the emission lines are relatively harp (10 nm).

While the NIR excitation of UCP particles addresses the problem of tissue light penetration, three remaining problems are: (1) elimination of systemic soluble porphyrin, (2) the efficient capture of photons and production of singlet oxygen, and (3) biocompatible delivery to the cancer site. We address these issues by presenting complex UCP core nanocrystals consisting of an inner UCP core, an intermediate coat of a tetraphenylporphyrin (TPP) which is excited by the up-converted 560 nm light generated by two 980 nm photons absorbed by the UCPs, and an outer layer of polyethylene glycol (PEG) which acts a solubilizing agent and also allows penetration of O_2 and diffusion of singlet oxygen. The PEG also serves to make the nanoparticles biocompatible and can be used for further chemical modification. The control of nanoparticle size is important because carriers with sizes between 100nm and 300 nm having a biocompatible PEG coating concentrate in cancer tissue using the defective endothelial cell lining of the vasculature in fast growing solid tumors [6]. This size-based targeting mechanism is termed Enhance Permeation and Retention (EPR).

2. Results

The core UCP nanocrystals are synthesized by a high temperature ligand exchange reaction[7] which produces nanoparticles of approximately 160 nm in diameter with a hydrophobic TOPOA (trioctyl phosphene-oleic acid) surface coating. The co-encapsulation of the UCP nanocrystals with the organic porphyrin sensitizer and a PEG protective layer to form the complex functional nanoparticle UCPs can be easily done in one step using our Flash NanoPrecipitation process[8]. The scheme for this assembly is presented in Fig. 1. The assembly process involves *O*(ms) rapid micromixing of a water-miscible organic stream

#103213 - $15.00 USD Received 27 Oct 2008; revised 8 Dec 2008; accepted 10 Dec 2008; published 22 Dec 2008

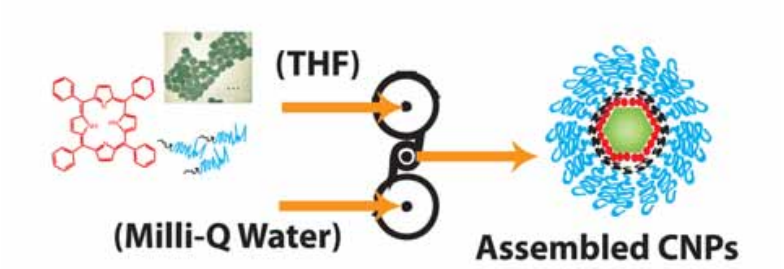

Fig. 1. Schematic representation of Flash NanoPrecipitation method for assembly of the composite nanoparticles incorporating the highly hydrophobic organic photosensitizer, tetraphenylporphyrin (red), 170-nm hexagonal NaYF4:Er3=,Yb^{3+} upconversion crystals (green) in a shell consisting of PEG(5k)-b-PCL(7k) amphiphilic block copolymer. All the constituents are initially dissolved or suspended in the organic phase, which is mixed at high speed against a large volume of water (10:1 water:THF), yielding the composite nanoparticle (CNP) structure shown right.

containing hydrophobic UCP particles, hydrophobic tetraphenylporphyrin (TPP) , and a block PEG copolymer (BPC) against a water stream as the anti-solvent. Producing supersaturations as high as 1000 in milliseconds initiates non-selective, diffusion limited aggregation and the formation of composite particles with the desired properties. Details of the CNP-UCP assembly can be found in Supplementary Materials. Briefly, the nanocrystals were suspended in THF at a concentration of 1.0 mg/ml, while the BCP consisted of a 7K hydrophobic polycaprolactone (PCL) block and 5K hydrophilic polyethylene glycol (PEG) block.

Analysis of the size distribution of the output of the micromixer using dynamic light scattering for various ratios of BCP:UCP:TPP is shown in Fig. 2. The uncoated UCPs are narrowly distributed with mean size of 160 nm. Addition of the TPP splits the distribution into two populations: a larger composite object with a size of 280 nm which is presumably the fully self-assembled composite nanoparticle (CNP) and smaller objects of roughly 60 nm which are presumably micelles formed by BCP surrounding a core of TPP. Since as the porphyrin concentration increases the porphyrin-only population gains higher and higher representation while the larger objects do not shift in size we surmise that the TPP photosensitizer forms a thin layer around the crystals, with all excess materials going to the porphyrin-only particles, that is, the nanocomposite 280 nm particles form a homogenous and well defined class of objects.

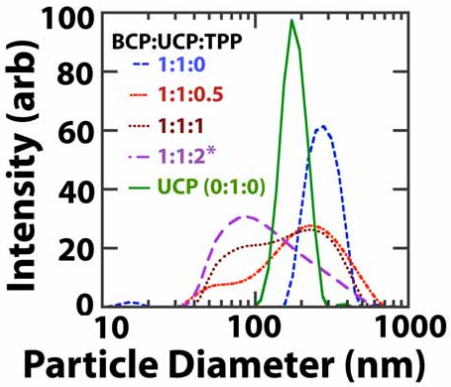

Fig. 2. Particle size distributions (normalized to constant area) for varying ratios of BCP:UCP:TPP in the turbulent micromixer. The initial distribution of the bare UCPs in hexane is the solid green line.

Figure 3 shows the emissions from crystals encapsulated in CNPs as well as the absorption spectrum for those particles.

#103213 - $15.00 USD Received 27 Oct 2008; revised 8 Dec 2008; accepted 10 Dec 2008; published 22 Dec 2008

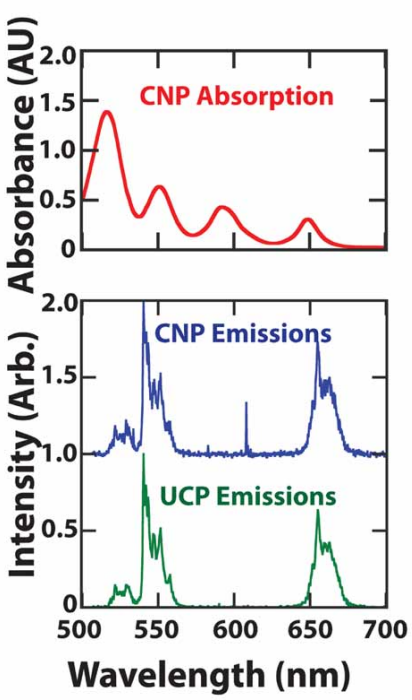

Fig. 3. Emission spectrum for upconversion crystals (lower spectrum) juxtaposed with absorption spectrum of tetraphenylporphine (TPP) photosensitizer (upper spectrum). Both spectra were collected from assembled nanoparticles rather than the components in an organic solvent, though the results were virtually identical for the latter case. Both spectra display strong, sharp peaks with overlap of the emission of the UCP and absorption by the TPP in the 550-nm region.

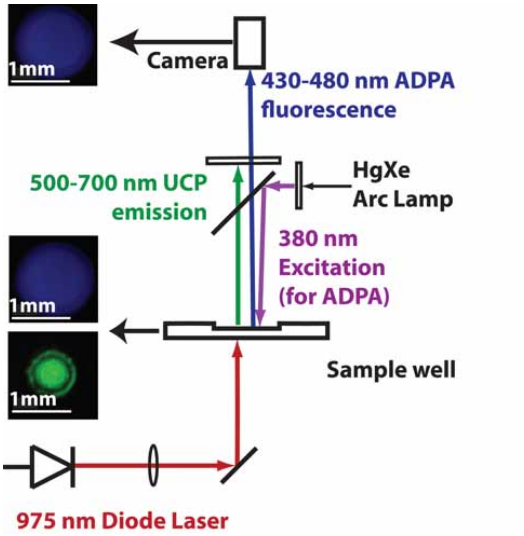

Fig. 4. Microscopy setup for the singlet oxygen production test using a fluorescent dye assay. Samples containing composite nanoparticles and the fluorescent dye ADPA were loaded into 1-mm wells drilled into glass microscope slides. The dye was imaged epifluorescently, with excitation at 380nm and emission collected from 430-480nm. IR excitation was delivered from below the well, with a 2.5 Watt infrared laser beam focused to a 0.3mm spot. UV and IR excitation light, as well as the visible emissions from the particles were filtered out and only the blue fluorescence signal from the ADPA was recorded for each sample.

The upconversion spectra display sharp peaks both as unprotected particles in THF and as

#103213 - $15.00 USD Received 27 Oct 2008; revised 8 Dec 2008; accepted 10 Dec 2008; published 22 Dec 2008

composite nanoparticles in water. The sharp emissions peaks are typical of rare earth upconversion materials and their emissions from atomic orbital transitions[9]. Overall brightness was attenuated by 50% to 90% upon polymer encapsulation. This effect was the most pronounced for high-BCP concentrations, (recipes with 6:1 and 3:1 polymer-to-crystal loading ratios), while low-block copolymer formulations (0.1:1 polymer:crystal) showed the least attenuation. The inclusion of porphyrin in the particles further diminished measured emissions intensity via absorption attenuation.

Following literature protocols [10, 11] singlet oxygen production by the CNPs was monitored in a solution containing the fluorescent dye 9,10-anthracenedipropionic acid (ADPA). The fluorescence of dye is quenched upon reacting with singlet oxygen, allowing the time course of singlet oxygen production to be monitored by tracking ADPA concentration. We used an epifluorescent microscopy setup to image the ADPA, while providing IR excitation from below the microscope stage, as depicted in Fig. 4. The method of photographing CNP-ADPA mixtures in glass microwells and then taking an average blue-channel or grayscale intensity proved to be a valid method for measuring ADPA concentration. Pixel intensity was linear in ADPA concentration for all CNP-ADPA preparations. Consequently, changes in average blue-channel or grayscale intensity were used to monitor ADPA concentration as a function of IR exposure time.

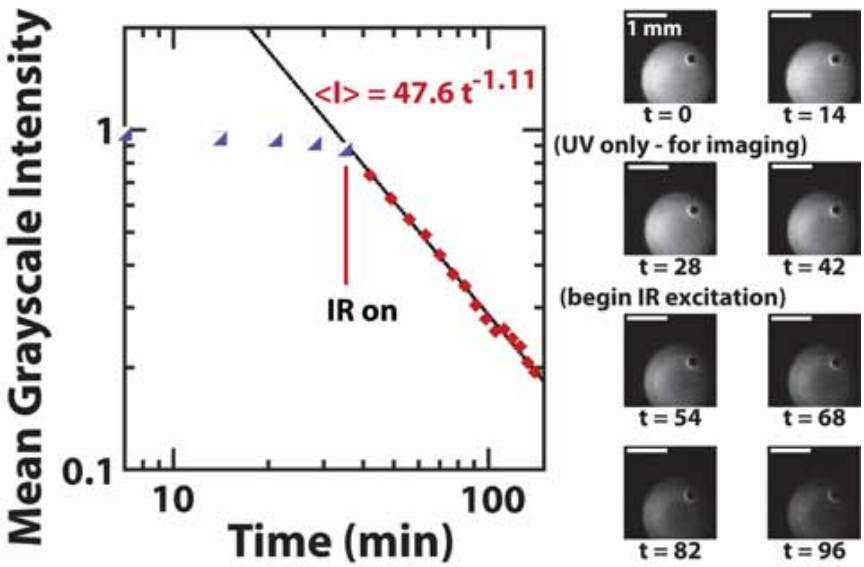

Fig. 5. Time course of ADPA bleaching during NIR-exposure. The right panel shows images from the first 98 minutes of testing, with minimal bleaching in the first three frames (no NIR input), and significant bleaching in the subsequent frames. This is illustrated in the curve in the left panel: the UV needed to image the ADPA dye leads to some baseline bleaching, but the ADPA bleaching takes on a markedly different rate under infrared illumination. We use a log-log scale, showing the power-law behavior of the bleaching.

Measurable, unambiguous infrared-initiated singlet oxygen production was observed using a composite nanoparticle recipe of 1:1:2 PEG-PCL:UCP:TPP in 3x PBS and 0.05g/L ADPA (100 micromolar). The sample was loaded in a glass microwell and immobilized by a glass cover slip (preparation of the well and sample described in Methods). A 5 second image of the well was captured once every 7 minutes, with a total UV exposure time of approximately 10 seconds per 7-minute cycle. For the first six cycles, no NIR excitation was provided. From minute 42 onward, 20 W/mm^2 of 975nm infrared light were delivered to the

#103213 - $15.00 USD Received 27 Oct 2008; revised 8 Dec 2008; accepted 10 Dec 2008; published 22 Dec 2008

well in 7-minute intervals, during NIR exposure the UV excitation was turned off. Figure. 5 plots the time course of the average image intensity over the 150 minutes of testing. The first four data points on Fig. 5 are controls with no NIR illumination, with only the 10 second illumination by the 380 nm probe beam to measure ADPA fluorescence. A minor amount of photobleaching from the probe beam is observed. However when the NIR illumination is initiated at 42 minutes a dramatic increase in the bleaching rate and hence singlet oxygen production is observed. As is evident when the bleaching kinetics are plotted as log(intensity) vs. time the bleaching decay is not a simple exponential but rather a clear power-law response with a slope of -1. This finding was consistent with the ADPA bleaching being a bimolecular reaction with the initial dissolved [O_2] concentration approximately the same as the [ADPA] concentration of 100 micromolar. If most of the change can be attributed to the IR illumination, this would correspond to an average ADPA bleaching rate of 1.1×10^3 mmol / L-min during the IR exposure period. Since the ADPA reaction will not capture all of the produced singlet oxygen, this serves as an underestimate of the singlet oxygen production rate. A control experiment was performed to compare singlet oxygen production in CNPs with and without porphyrin. The particles without TPP showed no bleaching of ADPA, indicating that the porphyrin is a necessary component of this system (data not shown).

3. Conclusion

We have demonstrated a functional prototype that co-localizes insoluble porphyrin with UCP crystals and efficiently generates singlet oxygen under NIR illumination. The application of UCP materials in photodynamic therapy is an attractive and active area. Chatterjee et. al [12] are the first to demonstrate folate receptor targeting with UCP nanoparticles. Their assembly approach of photosensitizer loading by adsorption into cationic poly(ethyleneimine) polymer coating produced loading levels of 1:15,000 photosensitizer:UCP crystal (weight basis), which is far lower than the 1:3 level that can be produced by our rapid precipitation process. Furthermore, the cationic PEI polymer is known to be cytotoxic in contrast to our PEG surface layer that is known to be biocompatible[13]. Zhang et. al have also produce PDT nanoparticles based on UCP nanoparticles[14]. Their process involves the trapping of photosensitizer in a thin silica layer deposited on the UCP nanoparticle surface. Their loadings of sensitizer are 1:219, and the bare silica layer on their nanoparticle surfaces are not expected to produce long-circulating nanoparticles. While the PEG coating applied by our Flash NanoPrecipitation process is biocompatible, studies on the biocompatibility of these UCP nanoparticle systems are underway. Also, the demonstration of delivery to tumor sites is also the subject of continuing studies. Particles of the size we have produced will lodge at the site of solid tumors by passing through defects in fast growing tumor vasculature by the EPR effect[15], and we have demonstrated the attachment of targeting ligands to the PEG chains in our nanoparticle constructs[16]. However, in vivo demonstration of targeting for these UCP nanoparticles is ongoing research. There are many questions that are still unresolved. The exact ratio of block copolymer, upconverting crystal, and porphyrin to maximize singlet oxygen production per IR photon is unknown. The attenuation of the emitted light from the UCP by the porphyrin coating and the kinetics and fate of singlet oxygen produced by the composite nanoparticle has not been modeled. Time- resolved fluorometry methods could enable the direct imaging of singlet oxygen. Beyond the physical characterization of the system, in vitro and in vivo efficacy studies are of high interest, especially in comparison to the efficacy of existing photodynamic therapies. Lastly, the therapeutic applications of the UCP-porphyrin pairing in a block- copolymer platform are further enhanced by the possibility of exciting the nanocrystals at X-ray wavelengths and the increased tissue penetration of that radiation. While this introduces the trade-off of incurring damage to tissue while initiating the PDT system, it also expands the applicability of PDT to almost any tissue and removes the limitations of optical penetration depth.

#103213 - $15.00 USD Received 27 Oct 2008; revised 8 Dec 2008; accepted 10 Dec 2008; published 22 Dec 2008

4. Methods

The UCP particles were made by the thermolysis method with trioctylphosphine/oleic acid as capping ligands[7]. The nanocrystals were received as a relatively dry, paste-like precipitate, and stored in a sealed polypropylene container at room temperature. The nanocrystals were suspended in tetrahydrofuran (THF), a water-miscible organic solvent, 1- 4 weeks after synthesis and drying. Nanocrystal aggregates were broken up with a probe-tip sonicator (Sonics and Materials Vibracell, Sonics and Materials Inc., Newtown, Connecticut), used at high power and 100% duty cycle for 15 minutes. Storage of the nanocrystals did not affect dispersibility within a month of synthesis. After two months, however the UCP crystals appeared to form larger irreversible aggregates. Once the UCP nanocrystals were successfully dispersed, block copolymer (PEG 5k-*b*- PCL 7k) and porphyrin were added to the suspension within half an hour of sonication. The polymer and organic additives were allowed to dissolve for 20-30 minutes before mixing. Synthesis of the particles was achieved using the Flash NanoPrecipitation method in a two-stream multi-inlet vortex mixer in keeping with the literature procedure [17].

Typical concentrations of the organic stream were 1mg/mL each of UCP nanocrystals, PEG-PCL, and TPP in reagent-grade THF (Aldrich). The organic stream was mixed against Milli-Q water (Millipore, Billerica, Massachusetts) at a 1:9 v/v THF:Water ratio. Both streams were injected into the mixer using electronically controlled syringe pumps (Harvard Apparatus, PHD 2000 programmable, Holliston, Massachusetts). The final compositions of the composite nanoparticle aqueous suspension were 0.01 to 1.0 0 wt% PEG-PCL, 0.10 wt% UCP, and 0.05- 0.20 wt% TPP. The assembled particles were then dialyzed against Milli-Q water in Spectra/Por dialysis bags, MWCO 6000-8000 Daltons (Spectrum Laboratories Inc., California) according to the prescribed method [18]. Because all particles were made with the same UCP loading, UCP crystal weight fraction will be given as a nominal indicator of composite nanoparticle concentration. The stability of mixed particles was assessed both visually and using dynamic light scattering (DLS). Particles not stabilized by block-copolymer formed large aggregates and were visibly turbid. Such visual observations were corroborated with large particle sizes in DLS measurements. UCP nanocrystals in THF, as well as undialyzed and dialyzed composite nanoparticles were measured using dynamic light scattering. The suspensions were typically diluted with additional THF or deionized water, as appropriate, to dilutions of approximately 10^{-3} wt% UCP – low enough to be in the range where multiple scattering does not influence the measured sizes. The particle sizes and size distributions in these diluted suspensions were measured with a DLS setup comprising: a Nd:YAG double-pumped continuous laser with output at 532nm and 50mW (Coherent Inc., Compass 315M-150mW, 320 micrometer beam, Santa Clara, California); and a photomultiplier tube at a 90-degree collection angle (Brookhaven Instruments, BI-200SM, Holtsville, New York). Data was communicated via a serial connection to an autocorrelator PC card and software program (ALV-Laser Vertriebsgesellschaft mbH, ALV-5000/E, Langen, Germany), which calculates particle size distributions based on decay time distributions assuming hard sphere behavior for the particle diffusivities (Stokes Law).

Acknowledgments

This work was supported by the AFOSR, NIH (HG01506), NSF Nanobiology Technology Center (BSCECS9876771), and NSF NIRT (CBET-0506966) . It was also performed in part at the Cornell NanoScale Science and Technology Facility (CNF) which is supported by the National Science Foundation under Grant ECS-9731293, its users, Cornell University and Industrial Affiliates.

#103213 - $15.00 USD Received 27 Oct 2008; revised 8 Dec 2008; accepted 10 Dec 2008; published 22 Dec 2008